NOTE

Magnetic Resonance in Medicine 00:000–000 (2013)

Use of Magnetization Transfer Contrast MRI to Detect Early Molecular Pathology in Alzheimer's Disease

Carlos J. Pérez-Torres,[1,2] Julia O. Reynolds,[2] and Robia G. Pautler[1,2,3,4]*

Purpose: The purpose of this study was to determine if magnetization transfer contrast (MTC) imaging could be used to detect early macromolecular accumulation in a mouse model of early Alzheimer's disease.

Methods: We obtained MTC images at 9.4 T at three different age points in the Tg2576 mouse model of Alzheimer's disease. The Tg2576 mouse exhibits increased amyloid beta deposition that eventually progresses into amyloid beta plaque formation, increased hyper-phosphorylated tau but does not exhibit neurodegeneration.

Results: Our results show an increase in the MTC signal that predates plaque formation and reported learning and memory deficits in the Tg2576 mouse. This increase in the MTC signal was reversed in a model of antioxidant therapy.

Conclusion: MTC magnetic resonance imaging can be used to detect early macromolecular changes in the Tg2576 mouse model of Alzheimer's disease. The source of the MTC contrast is likely complex and warrants further investigation in additional preclinical models that represent early and late stage Alzheimer's disease pathologies. **Magn Reson Med 000:000–000, 2013. © 2013 Wiley Periodicals, Inc.**

Key words: magnetization transfer; MRI; amyloid beta; Alzheimer's disease

Alzheimer's disease (AD), the most common form of dementia, is an incurable and progressive neurodegenerative disease (1). One of the major problems in the management of AD is the lack of a definitive premortem diagnostic test. The traditional approach that is used for AD diagnosis is through analysis of symptoms, clinical history, and family history. However, AD's primary early symptom, short-term memory loss, is not unique to the disease. Another common approach is to use noninvasive imaging to identify areas of neurodegeneration. With magnetic resonance imaging (MRI), it is possible to quantify the volume of brain structures and it has been established that AD patients have reduced hippocampal and total brain volumes (2). More recent reports suggest that changes in regional brain volume may be present as early as 10 years before clinically diagnosable AD symptoms (3). These findings reinforce the need for earlier diagnostic paradigms. Brain atrophy caused by neurodegeneration is a critical source for symptoms and is considered irreversible.

The best standard for definitive diagnosis has been postmortem pathology. The two pathophysiological hallmarks of AD first identified by Alois Alzheimer over 100 years ago are amyloid plaques and neurofibrillary tangles. Both of these molecular pathology hallmarks predate and may contribute to neurodegeneration (4). However, detecting either of these hallmarks in vivo has proven difficult. The biggest focus has been on imaging amyloid plaques, which hold promise as a more specific diagnostic factor. The most notable work in plaque imaging has been the development of the Pittsburgh Compound B agent (5) for positron emission tomography, though various MRI approaches have also been suggested (6–9). Most of the MRI approaches focused on either natural iron accumulation in the plaques (6) or MRI contrast agents (7–10) but, to date, these approaches typically understated the presence of plaques.

Macromolecular accumulation inclusive of amyloid beta, tau protein and likely additional proteins occurs well before plaque formation and neurodegeneration is believed to be a causative factor in AD (11). Therefore, imaging strategies that can detect early macromolecular accumulation before plaque formation and neurodegeneration would be extremely beneficial for both the diagnosis and monitoring of AD. Importantly, detection of preplaque macromolecular burden could lead to earlier detection of AD than any other previously mentioned approach. Previously, plasma (12,13) and cerebrospinal fluid (14,15) amyloid burden have been studied with mixed results. However, these are both indirect measurements of AD pathology. Furthermore, a recent study on familial AD patients found changes in the amyloid burden in cerebrospinal fluid as early as 25 years before symptoms and 10 years before amyloid plaque formation (16). Imaging macromolecular accumulation that occurs before plaque formation and neurodegeneration directly in the areas of the brain known to be affected earliest in AD such as the cortex (17) or the hippocampus (18,19) may provide an strategy for early detection of AD.

Magnetization transfer contrast (MTC) is a MRI technique to specifically detect changes in macromolecule concentration and composition (20). Clinically, MTC is most commonly used to track changes in myelination as way to grade multiple sclerosis lesions (21). The technique uses the application of a radiofrequency pulse at a

[1]Interdepartmental Program in Translational Biology and Molecular Medicine, Baylor College of Medicine, Houston, Texas, USA.

[2]Department of Molecular Physiology and Biophysics, Baylor College of Medicine, Houston, Texas, USA.

[3]Department of Neuroscience, Baylor College of Medicine, Houston, Texas, USA.

[4]Department of Radiology, Baylor College of Medicine, Houston, Texas, USA.

Grant sponsor: NIH; Grant number: R01AG029977; Grant sponsor: Mitchell Foundation, Anonymous Foundation.

*Correspondence to: Robia G. Pautler, Ph.D., Baylor College of Medicine, One Baylor Plaza, MS:335, Houston, TX 77030. E-mail: rpautler@bcm.edu

Received 16 November 2012; accepted 9 January 2013

DOI 10.1002/mrm.24665

Published online in Wiley Online Library (wileyonlinelibrary.com).

specific distance from the water resonance: the offset frequency. This radiofrequency pulse causes a loss of signal intensity proportional to macromolecular concentration. When combined with a reference image where the radiofrequency pulse is not applied, the percent of signal loss can be quantified in what is referred to as the magnetization transfer ratio (MTR). Specifically, MTC evaluates changes in semisolid macromolecules (22).

We hypothesized that the early accumulation of macromolecules in the Tg2576 mouse model of AD would have MTC effects. At the molecular level, both amyloid and tau begin as soluble monomers that eventually become insoluble deposits (19,23). The aggregation and eventual insolubility of these peptides suggests that the partially insoluble intermediates might provide an MTC effect. The focus of the study was on the two areas affected early in AD mentioned above: cortex and hippocampus.

In this work, we show that MTC MRI can detect AD-related macromolecular changes in the Tg2576 mouse model of AD. The Tg2576 mouse overexpresses a mutated form of amyloid precursor protein with the Swedish familial AD mutation and exhibits accumulation of detergent-insoluble amyloid as early as 6 months and eventual plaque formation as early as 10 months of age (24). This mouse model of AD was chosen because it does not present the advanced hallmarks of AD such as neurofibrillary tangles and neurodegeneration and is regarded as an "early" model of AD (24). However, phosphorylated tau has been observed in this model suggesting that some tau pathology is present (25–29). We were able to observe an MTC signal increase before plaque formation in this mouse model. When the Tg2576 mouse model was combined with a treatment paradigm known to reduce amyloid accumulation and plaque formation, tau pathology, and learning and memory deficits (28,30), the MTC signal went back to baseline. This imaging strategy has the potential to serve as an early imaging biomarker for AD before plaque development and neurodegeneration ensue.

METHODS

Animal Model

The Tg2576 mouse (24) overexpresses a mutant variant of the human APP gene ($Lys^{670} \rightarrow Asn^{670}$, $Met^{671} \rightarrow Leu^{671}$) found in a Swedish family with early-onset AD. Aged (12 months) Tg2576 mice ($N = 4$) and control littermates ($N = 5$) were used in the first part of the experiments. Longitudinal imaging at 4, 6, and 10 months was accomplished using the same model with transgenic mice ($N = 5$) and control littermates ($n = 4$).

The Tg/SOD mice overexpress both a mutant APP transgene as well as a mitochondrial superoxide dismutase (SOD2) transgene (28,30). To produce Tg/SOD mice, male Tg2576 mice were crossed with female SOD2 mice (31). This breeding scheme also produces Tg2576, SOD2 and WT siblings. We performed MTC imaging on aged (11–14 months) mice with Tg/SOD ($N = 3$), Tg2576 ($N = 2$), and Controls ($N = 3$) from this colony. All the animals used in this study were handled in compliance with institutional and national regulations and policies. The protocols were approved by the Institutional Animal Care and Use Committee at Baylor College of Medicine.

Imaging Protocol

Mice were anesthetized by isoflurane gas at 5% in oxygen and placed into a mouse holder where they were kept under anesthesia at a nominal 2% isoflurane in oxygen. Imaging was performed utilizing a Bruker Avance Biospec, 9.4 T spectrometer; 21 cm bore horizontal imaging system (Bruker Biospin, Billerica, MA) with a 35 mm volume resonator. During imaging, the animal body temperature was maintained at 37.0°C using an animal heating system (SA Instruments, Stony Brook, NY). T_2 weighted images were taken before MTC imaging to locate ideal MTC slice placement. MTC imaging pulse sequence comprised a presaturation square pulse at the designated offset frequency followed by a RARE sequence with echo time/pulse repetition time = 8.14/1512 msec with Rare Factor = 8. Images were recorded with a 256 × 256 matrix, field of view = 2 × 2 cm, slice thickness = 1 mm, and average = 2. Presaturation off-resonance pulses ranged from 0 to 20 kHz in the initial experiments but only the 20 kHz offset was used in subsequent experiments. Specific MT parameters were pulse length = 40 msec, number of pulses = 36, pulse strength = 6 or 12 μT, and saturation time = 1440 msec. A reference image was also taken with the same parameters except the saturation pulse.

An additional T_2 weighted image of the MTC slice was taken to visualize the anatomy. Regions of interest (ROIs) were manually drawn for each mouse on this T_2 weighted image of the hippocampus and cortex. Drawing the ROIs on the T_2 image ensured that that the MTR image would not bias ROI selection. For the hippocampus, the effort was made to try to avoid including the dorsal third ventricle. For the cortex, the ROI did not extend beyond the somatosensory cortex on either side. Average MTR measurements were calculated based on these ROIs.

Image and Statistical Analysis

MTRs in the form of MTR = (Unsaturated − Saturated)/Unsaturated were calculated. Pixel by pixel MTR calculations were performed using in house code developed in Matlab (The Mathworks, Natick, MA) to generate pseudocolored images. Region based MTR calculations were also performed in Matlab for quantification. Graphs and statistical analyses were conducted on the region-based calculations with Prism (GraphPad Software, San Diego, CA). Graphs are shown as Mean ± SEM.

RESULTS

Magnetization Transfer Contrast in Aged Tg2576 Mice

The initial focus was to assess whether both the MTR value would change in Tg2576 mice and at which frequency offset that change occurred. An age point that mimicked clearly symptomatic AD where changes would likely be more pronounced would be ideal for the initial validation. Specifically, experiments were conducted on 12-month-old Tg2576 mice because at this age point they

have a very consistent amyloid plaque pathology (24,32,33). Additionally, extensive learning and memory (24,30,33–35) and neurological deficits (28,36–38) have been reported at this age point.

Single slice MTC datasets and T_2-weighted anatomical reference images were acquired. ROIs were manually drawn on the anatomical reference image of each individual mouse for the cortex and hippocampus. These two regions were chosen because they are part of the earliest and most extensively affected by the AD molecular pathology. ROI based quantification of the MTC datasets was performed for the cortex (shown in Fig. 1A) and hippocampus (shown in Fig. 1B) at five different frequency offsets. The lower offsets have a higher MTR value due to nonspecific direct water saturation. For both regions, the largest enhancement in the Tg2576 mice over control littermates was at the 20 kHz offset. A one-tailed *t*-test was performed at this offset only and was found to be significant for both ROIs. The *P*-value for the cortex was 0.018 and for the hippocampus was <0.01. Figure 1C shows a representative MTR map and corresponding anatomical reference for each genotype. Images were manually aligned for ease of comparison.

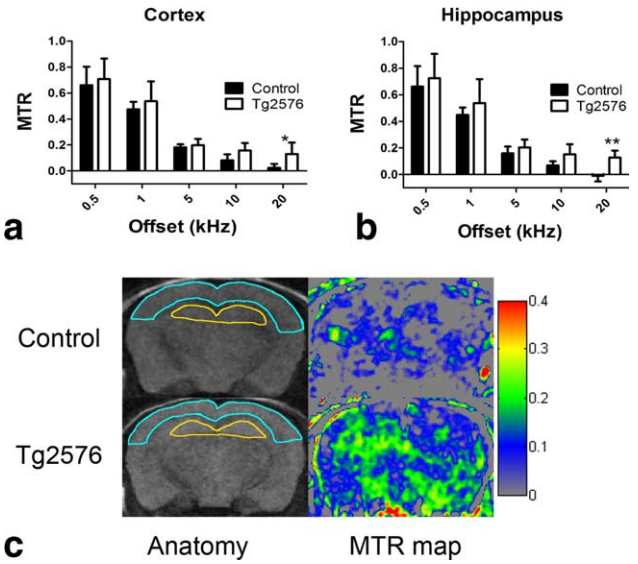

FIG. 1. MTC MRI values are elevated at 12 months in Tg2576 mice. Panels (**a**) and (**b**) show region based quantification of the MTR at 6 μT for the cortex and hippocampus, respectively. The genotypes were found to be significantly different in each case by two-way ANOVA. Student's *t* test were performed on the 20 kHz offset only and gave $P = 0.0305$ for panel (a) and $P < 0.01$ for panel (b), respectively. Number of animals equals 5 for control and 4 for Tg2576. Panel (**c**) shows a representative anatomical image and MTR map for each genotype. Representative ROIs for the cortex (light blue) and hippocampus (yellow) have been overlayed on the anatomical images.

Application as an Early Neuroimaging Biomarker

After establishing that MTC could distinguish between Tg2576 mice and littermate controls, the focus shifted toward determining the earliest time point at which MTR changes occurred. A cohort of Tg2576 mice and littermate controls were imaged at 4, 6, and 10 months longitudinally. At 4 months of age, Tg2576 mice are considered to be phenotypically identical to control mice. The 6-month time point was chosen because that is when accumulation of amyloid is first seen in this mouse model (32) and learning and memory deficits are not evident yet at 6 months (24). At 10 months of age, senile plaques are first detectable. Additionally, by this time, learning and memory as well as neurological deficits are already established (30,32,37). Overall, this provides three different scenarios similar to the earliest stages of AD: normal function, prodromal, and mild cognitive impairment.

MTC datasets were acquired at the 20 kHz offset based on the results in the 12-month-old mice. Single slice MTC datasets and T_2-weighted anatomical reference images were acquired. ROIs were manually drawn on the anatomical reference image of each individual mouse for the cortex and hippocampus. The average MTR for the cortex (shown in Fig. 2A) and hippocampus (shown in Fig. 2B) was calculated at each time point. As expected, there was no significant difference for either region at 4 months of age. The MTR values were significantly higher in both regions at 6 months of age as determined by one-tailed Student's *t*-test: *P*-value for the cortex was 0.013 and for the hippocampus was <0.01. This is at least 4 months before plaques develop in this mouse model. The MTR values were also elevated at 10 months. One-tailed Student's *t*-test once again confirmed that the difference was significant. The *P*-value for the cortex was <0.01 and for the hippocampus was 0.039. Figure 2C shows a representative MTR map and corresponding anatomical reference for each genotype at 4 months. Figure 2D shows the MTR map and corresponding anatomical reference for the same animals as Figure 2C at 10 months. Images were manually aligned for ease of comparison.

The MTC Signal Reverts to Baseline upon Efficacious Treatment

Additionally, we tested if the MTC signal changes in response to antioxidant therapy in Tg2576 mice. Our group has previously shown that when the Tg2576 mouse model of AD is crossed with a mouse overexpressing the mitochondrial antioxidant superoxide dismutase 2 (SOD), the resultant offspring (Tg/SOD) have reduced AD pathology including improved cognition, improved axonal transport, and improved cerebral blood flow (28,30). The MTR at 12 μT was calculated at the cortex for 11–14-month-old Tg2576 and Tg/SOD mice as shown in Figure 3. SOD overexpression recovered the increased MTC signal suggesting that it may be reflecting the therapeutic effect. These data suggest that this methodology can be used to assess therapeutic response in the Tg2576 mouse.

DISCUSSION

Diagnosis of AD is still a critical area of need with most diagnoses given by process of elimination. While other imaging paradigms are sufficient to track disease progression, they are currently ineffective at detecting the earlier stages of AD. The goal of this study was to test if MTC

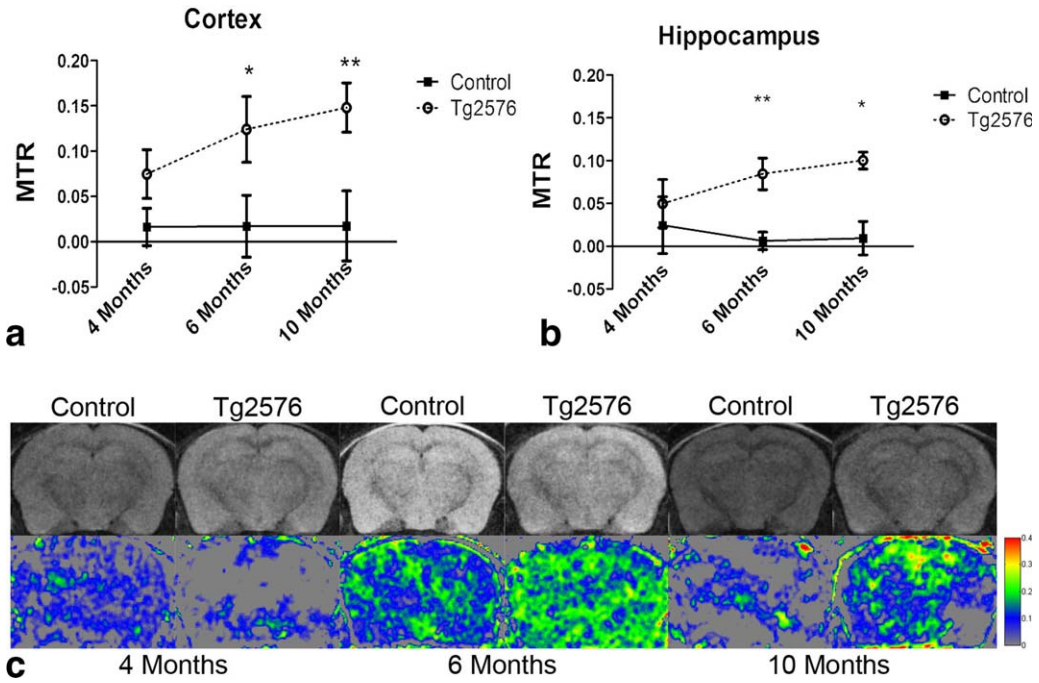

FIG. 2. MTC MRI values are elevated as early as 6 months in Tg2576 mice. Panels (**a**) and (**b**) show region based quantifications of the MTR at 6 μT for the cortex and hippocampus, respectively, at the 20 kHz offset. The same mice were imaged at each age point. The genotypes were found to be significantly different in each case by repeated measures ANOVA. Student's *t*-test were performed for each individual age point. $^{*}P < 0.05$ and $^{**}P < 0.01$. Number of animals equals 4 for control and 5 for Tg2576. Panels (**c**) and (**d**) present a representative anatomical image and MTR map of the same mouse for each genotype at 4 months in panel (c) and 10 months in panel (d), respectively.

MRI is sensitive to macromolecular changes that are seen early in AD. The results show that MTC MRI can detect differences in the Tg2576 mouse model well before plaque formation and learning and memory deficits. This is significant because no other MRI imaging modality has been reported to detect this earliest stage of AD (5). Importantly, the increased MTR in the Tg2576 mouse reversed back to baseline in the antioxidant treatment model. Therefore, we believe MTC MRI may be used in the Tg2576 model to examine response to treatment.

It will be important to identify the molecular source of the increased MTR. The two major molecular hallmarks of AD, and therefore likely contributing sources of the MTC signal, are amyloid beta and tau protein (4). However, there are other molecular pathologies that could also be involved including gliosis (39), vascular alterations (28,40), and cytoskeletal rearrangements (28,41). It would be ideal to test each individual possibility individually to identify how much it contributes to changes in the MTC signal but that will be challenging to do in vivo. Therefore, verification of these results in the Tg2576 in other mouse models of AD will be necessary to ensure the result is not restricted to the Tg2576 model. For example, in the case of tau pathology, the Tg2576 is not the ideal model and better models of tau aggregation will be needed to evaluate the contributions of tau accumulation (42,43). The Tg2576 mouse model used here only has limited tau pathology and does not exhibit neurodegeneration unlike that which is observed in AD patients. Animal models that include all three pathological hallmarks (amyloid beta, tau, and neurodegeneration) may be more accurate predictors of the usefulness of MTC. Such additional models would allow for consolidation of our findings compared with the reported clinical MTC data for AD patients. Specifically, symptomatic AD patients (late stage) show a lower MTR

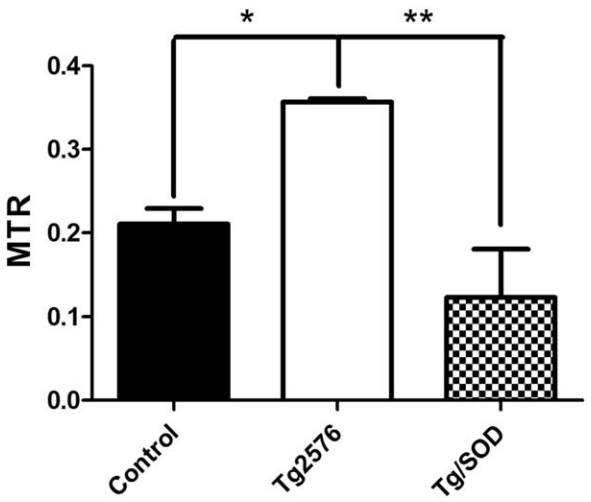

FIG. 3. The MTC signal can reflect a response to treatment. It shows the region based quantification of the MTR at 12 μT for the cortex at the 20 kHz offset for control, Tg2576, and Tg2576 crossed to SOD2 (Tg/SOD). The Tg/SOD mice have been previously shown to recover Tau phosphorylation (28). The genotypes were found to be significantly different by one-way ANOVA. Bonferroni post-tests were used to compare the Tg2576 group to WT and Tg/SOD. $^{*}P < 0.05$ and $^{**}P < 0.01$.

than controls (44,45). This lowered MTR is likely due to neurodegeneration and subsequent loss of macromolecules. Additionally, as neurons die they are replaced by cerebrospinal fluid which has a much lower MTR.

In summary, we have shown that the MTR is significantly increased in the Tg2576 mouse model, a model of early AD that exhibits amyloid beta accumulation, tau hyperphosphorylation, and no neurodegeneration. These data demonstrate that MTR can detect macromolecular changes in a mouse model of early stage AD and that MTC imaging should be further evaluated in additional, more complex models of AD to better define the clinical potential.

ACKNOWLEDGMENTS

Interdepartmental Program in Translational Biology and Molecular Medicine is funded in part by the Howard Hughes Medical Institutes Med into Grad Initiative. This work was funded by NIH (R.G.P.), the Mitchell Foundation (R.G.P.), and an Anonymous Foundation (R.G.P.).
Author contributions: C.J.P.-T. designed and performed experiments, analyzed data, and wrote the manuscript. J.O.R. performed experiments. R.G.P. designed experiments and helped to write the manuscript.

REFERENCES

1. Alzheimer's Association. 2011 Alzheimer's disease facts and figures. Alzheimers Dement 2011;7:208–244.
2. Laakso MP, Soininen H, Partanen K, Helkala EL, Hartikainen P, Vainio P, Hallikainen M, Hänninen T, Riekkinen PJ Sr. Volumes of hippocampus, amygdala and frontal lobes in the MRI-based diagnosis of early Alzheimer's disease: correlation with memory functions. J Neural Transm Park Dis Dement Sect 1995;9:73–86.
3. Tondelli M, Wilcock GK, Nichelli P, De Jager CA, Jenkinson M, Zamboni G. Structural MRI changes detectable up to ten years before clinical Alzheimer's disease. Neurobiol Aging 2012;33:825.e25-825.e36.
4. Querfurth HW, LaFerla FM. Alzheimer's disease. N Engl J Med 2010;362:329–344.
5. Klunk WE, Engler H, Nordberg A, et al. Imaging brain amyloid in Alzheimer's disease with Pittsburgh compound-B. Ann Neurol 2004;55:306–319.
6. Benveniste H, Einstein G, Kim KR, Hulette C, Johnson GA. Detection of neuritic plaques in Alzheimer's disease by magnetic resonance microscopy. Proc Natl Acad Sci USA 1999;96:14079–14084.
7. Poduslo JF, Wengenack TM, Curran GL, Wisniewski T, Sigurdsson EM, Macura SI, Borowski BJ, Jack CR. Molecular targeting of Alzheimer's amyloid plaques for contrast-enhanced magnetic resonance imaging. Neurobiol Dis 2002;11:315–329.
8. Wadghiri YZ, Sigurdsson EM, Sadowski M, et al. Detection of Alzheimer's amyloid in transgenic mice using magnetic resonance microimaging. Magn Reson Med 2003;50:293–302.
9. Yang J, Wadghiri YZ, Hoang DM, Tsui W, Sun Y, Chung E, Li Y, Wang A, de Leon M, Wisniewski T. Detection of amyloid plaques targeted by USPIO-A[beta]1-42 in Alzheimer's disease transgenic mice using magnetic resonance microimaging. Neuroimage 2011;55:1600–1609.
10. Petiet A, Santin M, Bertrand A, et al. Gadolinium-staining reveals amyloid plaques in the brain of Alzheimer's transgenic mice. Neurobiol Aging 2012;33:1533–1544.
11. Shankar GM, Li S, Mehta TH, et al. Amyloid-beta protein dimers isolated directly from Alzheimer's brains impair synaptic plasticity and memory. Nat Med 2008;14:837–842.
12. Fukumoto H, Tennis M, Locascio JJ, Hyman BT, Growdon JH, Irizarry MC. Age but not diagnosis is the main predictor of plasma amyloid beta-protein levels. Arch Neurol 2003;60:958–964.
13. van Oijen M, Hofman A, Soares HD, Koudstaal PJ, Breteler MM. Plasma AB1-40 and AB1-42 and the risk of dementia: a prospective case-cohort study. Lancet Neurol 2006;5:655–660.
14. Van Nostrand WE, Wagner SL, Shankle WR, Farrow JS, Dick M, Rozemuller JM, Kuiper MA, Wolters EC, Zimmerman J, Cotman CW. Decreased levels of soluble amyloid beta-protein precursor in cerebrospinal fluid of live Alzheimer disease patients. Proc Natl Acad Sci USA 1992;89:2551–2555.
15. Kester MI, Scheffer PG, Koel-Simmelink MJ, et al. Serial CSF sampling in Alzheimer's disease: specific versus non-specific markers. Neurobiol Aging 2012;33:1591-1598.
16. Bateman RJ, Xiong C, Benzinger TLS, et al. Clinical and biomarker changes in dominantly inherited Alzheimer's disease. New Engl J Med 2012;367:795-804.
17. Thal DR, Rüb U, Orantes M, Braak H. Phases of Aβ-deposition in the human brain and its relevance for the development of AD. Neurology 2002;58:1791–1800.
18. Braak H, Braak E. Neuropathological staging of Alzheimer-related changes. Acta Neuropathol 1991;82:239–259.
19. Jucker M, Walker LC. Pathogenic protein seeding in alzheimer disease and other neurodegenerative disorders. Ann Neurol 2011;70:532–540.
20. Wolff SD, Balaban RS. Magnetization transfer contrast (MTC) and tissue water proton relaxation in vivo. Magn Reson Med 1989;10:135–144.
21. Horsfield MA. Magnetization transfer imaging in multiple sclerosis. J Neuroimaging 2005;15:58S–67S.
22. Henkelman RM, Stanisz GJ, Graham SJ. Magnetization transfer in MRI: a review. NMR Biomed 2001;14:57–64.
23. Perl DP. Neuropathology of Alzheimer's disease. Mt Sinai J Med 2010;77:32–42.
24. Hsiao K, Chapman P, Nilsen S, Eckman C, Harigaya Y, Younkin S, Yang F, Cole G. Correlative memory deficits, Abeta elevation, and amyloid plaques in transgenic mice. Science 1996;274:99–102.
25. Tomidokoro Y, Harigaya Y, Matsubara E, Ikeda M, Kawarabayashi T, Shirao T, Ishiguro K, Okamoto K, Younkin SG, Shoji M. Brain Aβ amyloidosis in APPsw mice induces accumulation of presenilin-1 and tau. J Pathol 2001;194:500–506.
26. Tomidokoro Y, Ishiguro K, Harigaya Y, Matsubara E, Ikeda M, Park J-M, Yasutake K, Kawarabayashi T, Okamoto K, Shoji M. Aβ amyloidosis induces the initial stage of tau accumulation in APPSw mice. Neurosci Lett 2001;299:169–172.
27. Melov S, Adlard PA, Morten K, Johnson F, Golden TR, et al. Mitochondrial oxidative stress causes hyperphosphorylation of Tau. PLoS One 2007;2:e536.
28. Massaad CA, Amin SK, Hu L, Mei Y, Klann E, et al. Mitochondrial superoxide contributes to blood flow and axonal transport deficits in the Tg2576 mouse model of Alzheimer's disease. PLoS One 2010;5:e10561.
29. Neelima BC. Effect of aged garlic extract on APP processing and tau phosphorylation in Alzheimer's transgenic model Tg2576. J Ethnopharmacol 2006;108:385–394.
30. Massaad CA, Washington TM, Pautler RG, Klann E. Overexpression of SOD-2 reduces hippocampal superoxide and prevents memory deficits in a mouse model of Alzheimer's disease. Proc Natl Acad Sci USA 2009;106:13576–13581.
31. Ho Y-S, Vincent R, Dey MS, Slot JW, Crapo JD. Transgenic models for the study of lung antioxidant defense: enhanced manganese-containing superoxide dismutase activity gives partial protection to B6C3 hybrid mice exposed to hyperoxia. Am J Respir Cell Mol Biol 1998;18:538–547.
32. Kawarabayashi T, Younkin LH, Saido TC, Shoji M, Ashe KH, Younkin SG. Age-dependent changes in brain, CSF, and plasma amyloid (beta) protein in the Tg2576 transgenic mouse model of Alzheimer's disease. J Neurosci 2001;21:372–381.
33. Westerman MA, Cooper-Blacketer D, Mariash A, Kotilinek L, Kawarabayashi T, Younkin LH, Carlson GA, Younkin SG, Ashe KH. The relationship between Abeta and memory in the Tg2576 mouse model of Alzheimer's disease. J Neurosci 2002;22:1858–1867.
34. Arendash GW, Gordon MN, Diamond DM, Austin LA, Hatcher JM, Jantzen P, DiCarlo G, Wilcock D, Morgan D. Behavioral assessment of Alzheimer's transgenic mice following long-term Abeta vaccination: task specificity and correlations between Abeta deposition and spatial memory. DNA Cell Biol 2001;20:737–744.

35. King DL, Arendash GW. Behavioral characterization of the Tg2576 transgenic model of Alzheimer's disease through 19 months. Physiol Behav 2002;75:627–642.
36. Chapman PF, White GL, Jones MW, et al. Impaired synaptic plasticity and learning in aged amyloid precursor protein transgenic mice. Nat Neurosci 1999;2:271–276.
37. Smith KDB, Kallhoff V, Zheng H, Pautler RG. In vivo axonal transport rates decrease in a mouse model of Alzheimer's disease. NeuroImage 2007;35:1401–1408.
38. Townsend M, Qu Y, Gray A, Wu Z, Seto T, Hutton M, Shearman MS, Middleton RE. Oral treatment with a γ-secretase inhibitor improves long-term potentiation in a mouse model of Alzheimer's disease. J Pharmacol Exp Ther 2010;333:110–119.
39. Terai K, Iwai A, Kawabata S, Sasamata M, Miyata K, Yamaguchi T. Apolipoprotein E deposition and astrogliosis are associated with maturation of β-amyloid plaques in βAPPswe transgenic mouse: implications for the pathogenesis of Alzheimer's disease. Brain Res 2001;900:48–56.
40. Kumar-Singh S, Pirici D, McGowan E, Serneels S, Ceuterick C, Hardy J, Duff K, Dickson D, Van Broeckhoven C. Dense-core plaques in Tg2576 and PSAPP mouse models of Alzheimer's disease are centered on vessel walls. Am J Pathol 2005;167:527–543.
41. Lindwall G, Cole RD. Phosphorylation affects the ability of tau protein to promote microtubule assembly. J Biol Chem 1984;259:5301–5305.
42. Janus C. Conditionally inducible tau mice—designing a better mouse model of neurodegenerative diseases. Genes Brain Behav 2008;7:12–27.
43. Maccioni RB, Farías G, Morales I, Navarrete L. The revitalized tau hypothesis on Alzheimer's disease. Arch Med Res 2010;41:226–231.
44. Ridha BH, Symms MR, Tozer DJ, et al. Magnetization transfer ratio in Alzheimer disease: comparison with volumetric measurements. Am J Neuroradiol 2007;28:965–970.
45. Ginestroni A, Battaglini M, Della Nave R, et al. Early structural changes in individuals at risk of familial Alzheimer's disease: a volumetry and magnetization transfer MR imaging study. J Neurol 2009;256:925–932.